Journal of Chemical Neuroanatomy xxx (xxxx) 102259

Contents lists available at ScienceDirect

Journal of Chemical Neuroanatomy

journal homepage: www.elsevier.com/locate/jchemneu

Synaptoporin and parathyroid hormone 2 as markers of multimodal inputs to the auditory brainstem

Stefan Reuss [a, 1, *], Denise Linsmayer [b], Julia Balmaceda-Braun [b], Julia von Rittberg [b], Stephanie Mitz [b], Ursula Disque-Kaiser [b], Ted Usdin [c], Rudolf E. Leube [d]

[a] Department of Nuclear Medicine, University Medical Center, Johannes Gutenberg-University, Mainz, Germany
[b] Department of Anatomy and Cell Biology, University Medical Center, Johannes Gutenberg-University, Mainz, Germany
[c] Systems Neuroscience Imaging Resource, National Institute of Mental Health, Bethesda, MD, USA
[d] Institute of Molecular and Cellular Anatomy, RWTH Aachen University, Aachen, Germany

ARTICLE INFO

Keywords:
Synaptic vesicle protein
Synaptoporin
Auditory system
TIP39
Superior olivary complex
Medial paralemniscal nucleus
Neuronal tracing
Phaseolus vulgaris leucoagglutinin
PTH2

ABSTRACT

The distribution of the synaptic vesicle protein synaptoporin was investigated by immunofluorescence in the central auditory system of the mouse brainstem. Synaptoporin immunostaining displayed region-specific differences. High and moderate accumulations of were seen in the superficial layer of the dorsal cochlear nucleus, dorsal and external regions of the inferior colliculus, the medial and dorsal divisions of the medial geniculate body and in periolivary regions of the superior olivary complex (SOC). Low or absent labeling was observed in the more central parts of these structures such as the principal nuclei of the SOC. It was conspicuous that dense synaptoporin immunoreactivity was detected predominantly in areas, which are known to be synaptic fields of multimodal, extra-auditory inputs. Target neurons of synaptoporin-positive synapses in the SOC were then identified by double-labelling immunofluorescence microscopy. We thereby detected synaptoporin puncta perisomatically at nitrergic, glutamatergic and serotonergic neurons but none next to neurons immunoreactive for choline-acetyltransferase and calcitonin-gene related peptide. These results leave open whether functionally distinct neuronal groups are accessed in the SOC by synaptoporin-containing neurons. The last part of our study sought to find out whether synaptoporin-positive neurons originate in the medial paralemniscal nucleus (MPL), which is characterized by expression of the peptide parathyroid hormone 2 (PTH2). Anterograde neuronal tracing upon injection into the MPL in combination with synaptoporin- and PTH2-immunodetection showed that (1) the MPL projects to the periolivary SOC using PTH2 as transmitter, (2) synaptoporin-positive neurons do not originate in the MPL, and (3) the close juxtaposition of synaptoporin-staining with either the anterograde tracer or PTH2 reflect concerted action of the different inputs to the SOC.

1. Introduction

Synaptoporin (also named synaptophysin II) is an integral component of the synaptic vesicle membrane. It is a member of the physin gene family that also includes the synaptic vesicle protein synaptophysin (Hübner et al., 2002). They have approximately 58 % sequence homology. They are characterized by four transmembrane domains with divergent cytoplasmic N- and C-termini (Betz, 1990; Knaus et al., 1990). In analogy to synaptophysin, the ~37 kDa synaptoporin is localized in synaptic vesicles and may have channel functions. It is, how-

Abbreviations: Aq, cerebral aqueduct; ChAT, choline acetyltransferase; CGRP, calcitonin gene-related peptide; CIC, central nucleus of the inferior colliculus; CN, cochlear nucleus; DCIC, dorsal cortex of the inferior colliculus; DCN, dorsal cochlear nucleus; DG, dentate gyrus; DPO, dorsal periolivary region; ECIC, external cortex of the inferior colliculus; Glu, glutamate; LL, lateral lemniscus; LSM, laser scanning microscope; LSO, lateral superior olive; MG, medial geniculate body; MGD, dorsal division of the medial geniculate body; MGM, medial division of the medial geniculate body; MNTB, medial nucleus of the trapezoid body; MPL, medial paralemniscal nucleus; MSO, medial superior olive; nNOS, neuronal nitric oxide synthase; PAG, periaqueductal gray matter; PTH2, parathyroid hormone 2; RT, room temperature; sl, superficial layer; SOC, superior olivary complex; SPN, superior paraolivary nucleus; VCN, ventral cochlear nucleus; VPO, ventral periolivary region; 5-HT, 5-hydroxytryptamine = serotonin; 7n, facial nerve

* Corresponding author.
E-mail addresses: reuss@uni-mainz.de (S. Reuss), deniselinsmayer@gmail.com (D. Linsmayer), Julia-Braun@gmx.de (J. Balmaceda-Braun), julia@rittberg.de (J. von Rittberg), smitz@uni-mainz.de (S. Mitz), disque@uni-mainz.de (U. Disque-Kaiser), usdint@mail.nih.gov (T. Usdin), rleube@ukaachen.de (R.E. Leube).
[1] orcid.org/0000-0003-1064-5067

https://doi.org/10.1016/j.jchemneu.2023.102259
Received 12 December 2022; Received in revised form 5 March 2023; Accepted 16 March 2023
0891-0618/

ever, thought to be "associated with specific pathways implicated in higher functions of the brain" (Marquèze-Pouey et al., 1991). In accordance, synaptoporin shows a more restricted distribution in comparison to synaptophysin, to which it generally co-localizes (Singec et al., 2002).

Previous studies reported differential synaptoporin expression in mammalian brain regions. Strong signals were detected using antibodies against the protein or in situ-hybridization in various cerebrocortical regions, hippocampal dentate gyrus, cerebellum, medial habenular nucleus, and hypothalamus and the superior and inferior colliculi (Fykse et al., 1993; Grabs et al., 1994; Knaus et al., 1990; Marquèze-Pouey et al., 1991). Synaptoporin was also observed in the spinal dorsal horn and in small dorsal root ganglion cells where it was upregulated upon peripheral nerve injury (Sun et al., 2006).

Dense synaptoporin staining was described in the inferior colliculus, the only auditory structure that has been examined to date (Marquèze-Pouey et al., 1991). We therefore conducted an initial study on the distribution of synaptoporin with emphasis on the auditory system. When the study was started, an antibody suitable for immunohistochemistry was not available. We therefore used a custom-made antibody and immunofluorescent detection. We found remarkable differences in synaptoporin staining density within the subcortical auditory system. The differential expression pattern of synaptoporin, particularly in the superior olivary nucleus (SOC) of the auditory brainstem, prompted us to focus on the periolivary regions, in particular the dorsal periolivary area (DPO).

Besides investigating the distribution of synaptoporin immunoreactivity in the SOC, we sought to determine which neuronal subtypes are contacted by synaptoporin-immunoreactive puncta. We therefore utilized double-immunofluorescence to study neurons characterized by immunolabeling for calcitonin gene-related peptide, choline-acetyltransferase, glutamate, neuronal nitric oxide-synthase and serotonin. These substances had been found previously in SOC neurons (Bartolomé and Gil-Loyzaga, 2005; Lu et al., 1987; Moore and Moore, 1987; Reuss, 1998; Safieddine and Eybalin, 1992).

Finally, we considered that synaptoporin might be a marker of extra-auditory input to the SOC region. Non-auditory afferents supposedly originating in brain regions such as raphe nuclei, locus ceruleus, tegmentum, or reticular formation are thought to contribute to the shaping of auditory functions (Mulders and Robertson, 2001). Serotonergic, noradrenergic and cholinergic fiber systems terminate in the SOC with mainly higher density in periolivary regions (Steinbusch, 1981; Thompson and Schofield, 2000), and several neuropeptides exert their influence on neurons located here (Wang and Robertson, 1997).

The periolivary region, further, is involved in the integration of multisensory information via its coupling to the medial paralemniscal nucleus (MPL). Most neurons in the MPL are characterized by expression of parathyroid hormone 2 (PTH2), originally designated as tuberoinfundibular peptide of 39 residues (TIP39; Dobolyi et al., 2002; Palkovits et al., 2004; Usdin et al., 1999; HUGO Gene Nomenclature Committee, https://www.genenames.org/data/gene-symbol-report/#!/hgnc_id/30828). The peptide is involved in the regulation of many neural functions such as nociception, thermoregulation, reproduction, and social interactions (cf. Dobolyi et al., 2010; Keller et al., 2022a; Keller et al., 2022b). The MPL is part of the audiogenic stress pathway, and neurons in the rat MPL expressing this peptide are activated by acoustic stress (Palkovits et al., 2009).

To clarify whether synaptoporin and PTH2 are present in related structures in the periolivary region and whether these peptides may originate in the MPL, we used various combinations of anterograde neuronal tracing upon injection into the MPL and immunofluorescent labelling of synaptoporin and PTH2. We now describe codistribution of the tracer and PTH2 in the DPO, and the close spatial relation of synaptoporin puncta to structures labeled by the tracer or the PTH2-antibody.

2. Material and methods

2.1. Animals and treatment

Animals were maintained at the animal facility of the Department of Anatomy and Cell Biology (University of Mainz) under constant conditions (light:dark 12:12 h, room temperature 21 ± 1 °C, food and water available ad libitum). The procedures concerning animals reported in this study complied with German and European laws for the protection of animals and were approved by the county-government office (Bezirksregierung Rheinhessen-Pfalz, Az 177–07/961–30). All efforts were made to minimize the number of animals and their suffering.

Five two-months-old male mice (C57BL/6N) were used for single-label immunofluorescence detection of synaptoporin. Double-label immunohistochemistry was conducted on six C57BL/6 N and six BalbC mice.

Neuronal tracing, combined with synaptoporin and/or PTH2-immunofluorescence, was conducted on nine two-months-old male Wistar rats (Janvier, France).

All animals were killed by ether overdose at the middle of the light-period and immediately perfused transcardially with phosphate-buffered 0.9 % saline (PBS, to which 15000 IU heparin/l were added) at room temperature (RT), followed by an ice-cold fixative (4 % paraformaldehyde, 1.37 % L-lysine, 0.21 % sodium-periodate in phosphate buffer (PLP; McLean and Nakane, 1974) at a constant rate of 25 ml/min (rats) or 5 ml/min (mice). The right atrium was opened to enable venous outflow.

2.2. Tissue processing and synaptoporin immunohistochemistry

The brains were removed, postfixed for 1 h, and stored overnight at 4°C in phosphate-buffered 30 % sucrose for cryoprotection. They were then serially sectioned at 30 μm thickness on a freezing microtome in the frontal plane. Sections were collected into four parallel sets in PBS and, for immunohistochemistry, free-floating incubated in PBS-diluted custom-made polyclonal antiserum raised in guinea pig and directed against the CGSSGGYSQQANLG-sequence of murine synaptoporin (PSL Peptide Specialty Laboratories GmbH, Heidelberg, Germany; see Table 1). Antibodies were isolated by affinity chromatography. Since synaptoporin-knockout animals were not available, we preabsorbed the antibodies with synthetic synaptoporin peptide. This procedure abolished immunosignals. Antibodies did not yield signals in Western blot preparations.

The incubation was conducted overnight at RT in PBS to which 1 % normal donkey serum and 0.1 % Triton-X 100 were added. After three rinses in PBS, the reaction was visualized using fluorescent-labeled IgG directed against the host species of the primary antibodies. As the detection system for synaptoporin antibody binding, we used Cy3 conjugated to an $F(ab)_2$ fragment of goat anti-guinea pig IgG.

2.3. Double-immunofluorescence of mouse superior olivary complex

In the double-labelling experiments, free-floating sections were simultaneously incubated with additional antibodies directed against calcitonin gene-related peptide, choline-acetyltransferase, glutamate, neuronal nitric oxide synthase, or serotonin. The antibodies had been used earlier in our laboratory and were characterized previously (e.g., Reuss et al., 2009). Details on the substances used for neuronal tracing and immunohistochemistry are given in Table 1. For the detection of these substances, Cy2 coupled to IgG directed against the host species of the respective primary antibody were applied.

Sections were mounted on gelatinized glass slides, dried, cleared in xylene, and cover-slipped with Merckoglas (Merck, Darmstadt, Germany). All materials were analyzed using an Olympus BX51 research microscope equipped with epifluorescence unit, highly specific single

Table 1
Substances used for the identification of MLP efferents and the characterization of transmitter substances. mc, monoclonal; pc, polyclonal; n/a, not available; RRID, Research Resource Identifier (https://antibodyregistry.org).

Substances	Abbreviation	Host	Dilution	Source	Cat#, Lot#, RRID
Neuronal tracer					
Phaseolus vulgaris-Leucoagglutinin	Pha-L		2.5 %	Vector, Burlingame, CA, USA	L111D, S1216,n/a
Primary antibodies					
Calcitonin gene-related peptide	CGRP	rabbit, pc	1:1000	Amersham, Hannover, Germany	C8198, n/a, AB_259091
Choline-acetyltransferase	ChAT	goat, pc	1:500	Chemicon, Temecula, USA	AB144P, 0702053325, AB_2079751
Glutamate	Glu	rabbit; pc	1.1000	Sigma, St. Louis, USA	G6642, 083H4826, AB_259946
Neuronal nitric oxide synthase	nNOS	rabbit, pc	1:1500	Progen, Heidelberg, Germany	16058, DS 7598, AB_1542573
Phaseolus vulgaris-Leucoagglutinin	Pha-L	rabbit, pc	1:1000	Vector	AS2300, T1024, AB_2313686
Serotonin	Ser	rat, mc	1:200	Chemicon	MAB 352, 2312540, AB_94865
Synaptoporin		guinea pig, pc	1:300	custom-made (see 2.2 for details)	
Synaptoporin		rabbit, pc	1:1000	Synaptic Systems, Göttingen, Germany	102002, 102002/8, AB_887841
Tuberoinfundibular Peptide of 39 Residues	TIP39	rabbit, pc	1:1000	custom-made. protein parathyroid hormone 2 (PTH2)	
Secondary antibodies					
Cy3-anti-guinea pig F(ab´)$_2$		donkey	1:400	Jackson, West Grove, PA, USA	706–166–148, 74309, AB_2340461
Cy2-anti-guinea pig F(ab´)$_2$		donkey	1:100	Jackson	706–266–148, 78461, AB_2340454
Cy3-anti-rabbit F(ab´)$_2$		donkey	1:400	Jackson	711–166–152, 81083, AB_2313568
Cy2-anti-rabbit F(ab´)$_2$		donkey	1:400	Jackson	711–226–152, 81285, n/a
Cy2-anti-goat F(ab´)$_2$		donkey	1:400	Jackson	705–226–147, 83321, n/a
Cy2-anti-rat F(ab´)$_2$		donkey	1:400	Jackson	712–226–153, 72611, n/a
Biotin-anti-rabbit F(ab´)$_2$		donkey	1:1000	Jackson	711–066–152, 90000, AB_2340594
Streptavidin-HRP		1:100	Rockland, Gilbertsville, PA, USA	DY998	
Cy3-tyramide		1:50	Bio-Techne, Wiesbaden, Germany	6457/1	

and dual band filter sets allowing the single or simultaneous excitation and observation of dyes without overlapping-artifacts (Olympus fluorescence monochromatic and dichromatic mirror cubes, maximal excitation/maximal emission, Cy2: 489/506 nm, Cy3: 552/565 nm). Photomicrographs (200 dpi) were taken with an Olympus ColorView-12 digital color camera employing the AnalySIS Software (Olympus Soft Imaging Solutions, Münster, Germany). Some images were converted into black-and-white to achieve higher contrast. The Adobe Photoshop and Powerpoint programs were used to overlay and arrange digital images, to adjust image contrast and brightness of whole images, and to add labels. Brain regions were identified using the stereotaxic brain atlases of mouse and rat (Paxinos and Franklin, 2013; Paxinos and Watson, 2014).

At least twenty sections per set from each animal group were used for double-immunofluorescence. Further sections were used for antigen distribution and antibody specificity tests.

2.4. Neuronal tracing

The intracerebral injection of neuronal tracer was conducted in rats at daytime under general anesthesia. This species was selected because of its larger brain size compared to mice. Surgery was initiated by isoflurane inhalation and then maintained by 5 mg/kg b.wt. of a mixture of 55 % ketamine (Ketavet, Pfizer, Berlin, Germany) and 45 % xylazine (Rompun, Bayer, Leverkusen, Germany) given intraperitoneal). If necessary, rats received 30 % of the initial dose to continue anesthesia after 25 min. Animals were placed under an infrared lamp to keep body temperature constant.

A stereotaxic unit was used to fix the anesthetized animal's head in a prone position. A medial incision of the scalp was made, and a small hole was drilled into the skull with a dental drill. After cutting the dura mater, a glass capillary (tip diameter < 1 µm) was inserted and the tracer was slowly pressure-injected. The injection methods were optimized in our laboratory and used in a number of tracing studies (e.g., Reuss, 2021; Reuss et al., 2016; Reuss and Decker, 1997; Reuss et al., 1999; Reuss et al., 2020). Methods included backfilling of the capillary, careful cleaning of the tip, and pulling back a small amount of fluid before insertion. Approximately 150 nl of the anterograde tracer Phaseolus vulgaris-leucoagglutinin (Gerfen and Sawchenko, 1984; Reuss and Decker, 1997) was injected into the MPL. The injection coordinates (Bregma −8.2 mm, 2.4 mm lateral to midline, 7.0 mm below brain surface) were taken from the rat brain atlas (Paxinos and Watson, 2014). After pulling back the capillary, the animals received supportive medical treatment including analgesia.

After five to seven days, rats were killed by anesthesia overdose and immediately perfused by the PLP fixative. Brains were marked on one side and processed as described above. Sections containing tracer injection sites were immediately mounted onto gelatin-coated slides, dried overnight and coverslipped with Merckoglas (Merck, Darmstadt, Germany) for injection site verification. To visualize tracing, free-floating sections were incubated with antibodies directed against Pha-L. Selected sections containing injection or target sites were counterstained with hematoxylin-eosin. Injection sites were delineated in a sketch showing MPL and neighboring structures (see Fig. 1 B).

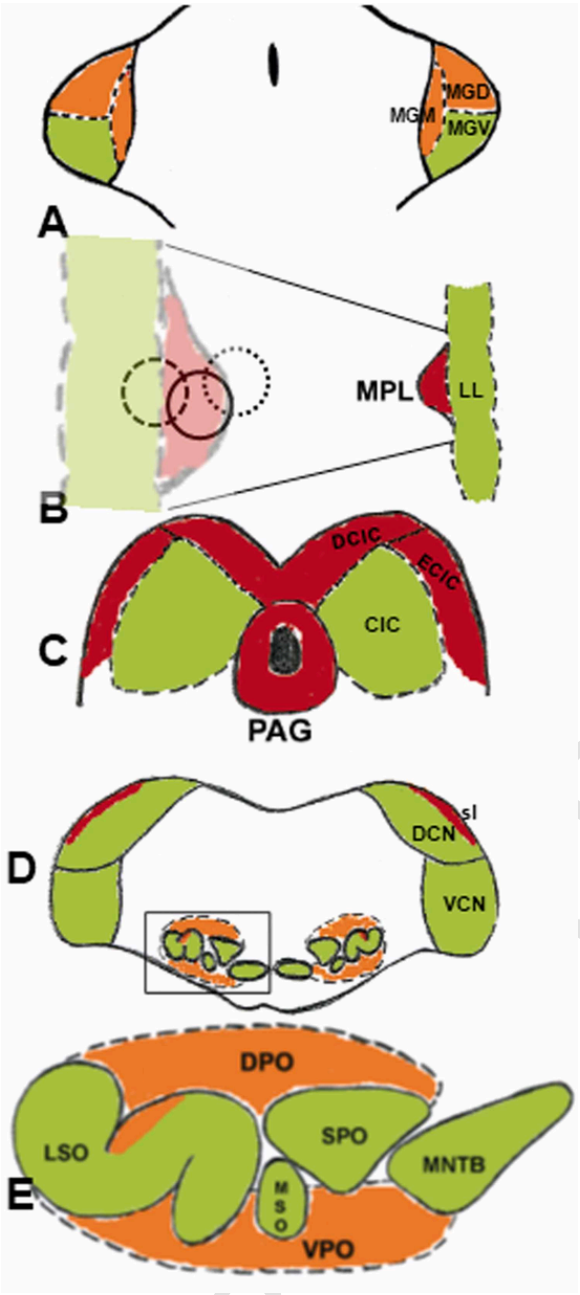

Fig. 1. Schematic presentation of synaptoporin-distribution in subcortical auditory structures of the mouse. Approximate levels with regard to Bregma are: (A) −3.2 mm (according to Figure 57 of the mouse stereotactic atlas (Paxinos and Franklin, 2013), (B) −4.6 mm (Figure 69) in mice (right side), (C) −5.1 mm (Figure 73), (D) −6.0 mm (Figure 81), and (E) −5.5 mm (Figure 77). The boxed region in D is shown in higher magnification in E. Note that the left side in B shows a higher magnification demonstrating three typical tracer injection sites in rats at the approximate level −8.3 (according to Figure 102 of the rat stereotactic atlas by Paxinos and Watson, 2014). Continuous line represents MPL injection, broken line injection into MPL and ventral group of lateral lemniscal nuclei located laterally to MPL, dotted line indicates injection into MPL and oral part of pontine reticular nucleus located medially to the MPL.

2.5. Combined Pha-L tracing and immunohistochemistry in rats

To test whether Pha-L injected into the MPL and PTH2 or synaptoporin colocalize in the superior olivary complex, we used double immunofluorescence. Unfortunately, our specificity tests showed that the guinea pig-raised synaptoporin antibody used in mice in the present study did not adequately label expected structures in rats. This was probably related to the fact that the amino acid asparagine (N) in mouse is, in rat, substituted by serine (S) in the peptide sequence against which the antibody was raised. Since commercially available antibodies raised in species other than rabbit did not meet our specificity requirements, we used a polyclonal synaptoporin antibody raised in rabbits (see Table 1).

Simultaneous incubations using two antibodies raised in the same species may be conducted under special conditions (cf. Warford et al., 2014), i.e., using fluorescence-coupled IgG for one of the antibodies and tyramide amplification in the detection of the other. Both antibodies were used in minimal concentrations that were titrated in pilot experiments, e.g., PTH2 was used at 1:16000 instead of 1:1000 in unamplified systems. For a preceding antigen retrieval, we mounted sections on Superfrost-plus slides (Merck) and incubated these in 10 mM citrate buffer (pH 6.0) at 96° C for 35 min. After cooling, sections were rinsed 3 × 10 min in 10 mM PBS and treated further as described above.

We conducted three different combinations of double-labelling using the tyramide signal amplification (TSA) method, originally introduced by Bobrow et al. (1992). In brief, TSA is based on tyramide converted by peroxidase to highly reactive tyramide radicals, which covalently bind to tyrosine-chains of near proteins. We used a biotinylated donkey anti-rabbit secondary antibody (1:1000 in PBS, 90 min, RT). After three rinses in PBS, sections were incubated in streptavidin-horseradish peroxidase complex (1:100 in PBS, 30 min, RT). After another rinse, sections were incubated in tyramide fluorescence complex (8 min, RT), which is converted by peroxidase in turn strengthening the immunohistochemical signal. After rinsing, sections were treated as described above.

Sections were first immunolabeled for PTH2 by using tyramide amplification and Cy3-visualisation, and then incubated with the synaptoporin antibody or the PhaL antibody, each marked with Cy2-conjugated secondary antibody. Selected sections were additionally studied using a TCS NT confocal scanning microscope equipped with an argon (488 nm) and a krypton (568) laser system for the excitation and detection of Cy2 and Cy3 (Leica, Wetzlar, Germany).

2.6. Control studies

Specificity studies, carried out by omitting primary or secondary antibodies, or by preabsorption of the antibodies with the respective immunogen, showed the absence of the fluorescent signal. We also conducted an extensive series of test-incubations to ensure that no cross-reactions between simultaneously used primary and/or secondary antibodies occurred. Care was, in particular, taken when two antibodies raised in the same species were used for double-immunofluorescence.

Tracing controls consisted of additional rats in which only areas outside the MLP, e.g. the medially located pontine reticular nucleus, were injected (see above). In these cases, Pha-L was not observed in the superior olivary region. Of note, no differentiated labeling was seen when the Pha-L antibody was used on brain sections obtained from animals that did not receive Pha-L injections.

3. Results

3.1. Synaptoporin localization in murine brain regions

We observed widespread but differential synaptoporin staining in neural regions of murine brain sections. For example, strong immunoreactivity was found in the cerebellar molecular layer, the granule layer of the hippocampal dentate gyrus and the superior colliculus. These findings confirm previous studies (Fykse et al., 1993; Grabs et al., 1994; Knaus et al., 1990; Marquèze-Pouey et al., 1991). Notably, we observed only punctate immunoreactivity in the regions studied, most probably representing presynaptic terminals (see 4.1.). No fibers or neuronal so-

mata were stained by the synaptoporin antibody. These findings are in line with the expected synaptic accumulation of synaptoporin in neurotransmitter-containing vesicles in the adult brain.

We then concentrated on the central subcortical auditory system. Considerable differences in the synaptoporin expression level, i.e., density of immunoreactive structures, were observed within the auditory nuclei (for a schematic overview see Fig. 1; examples are given in Figs. 2 and 3). Highest staining density was found in the medial paralemniscal nucleus, dorsal and external cortical regions of the inferior colliculus and in the superficial layer of the dorsal cochlear nucleus. Moderate to high labelling density was observed in the medial geniculate body and periolivary regions of the superior olivary complex. Low or absent synaptoporin immunoreactivity was observed in the ventral division of the medial geniculate body, the nuclei of the lateral lemniscus, the central part of the inferior colliculus, in cochlear nuclei, and in principal nuclei of the SOC.

As seen in frontal sections arranged from anterior to posterior, the medial geniculate exhibited moderate to high synaptoporin labelling. The immunoreactivity was often present in clusters in the dorsal, medial and dorsal divisions of the medial geniculate, while the ventral aspect was almost devoid of synaptoporin reactivity (Figs. 1A, 2AB).

The medial paralemniscal nucleus exhibited high density synaptoporin staining, which extended dorsally and ventrally into the lateral lemniscus (Figs. 1 B, 6C). The lateral lemniscus was otherwise unlabeled or exhibited only scarce labelling.

Central aspects of the inferior colliculus were only scarcely stained, while its cortical regions exhibited moderate to high density of synaptoporin immunoreactivity. In particular, the outer laminae of the dorsal and external cortices exhibited dense immunoreactivity while the underlying laminae were less stained (Fig. 2 CD). Moderately dense staining was observed in the region neighboring the dorsal roof of the cerebral aqueduct, extending into the lateral and ventral parts of the periaqueductal grey (Fig. 2 C).

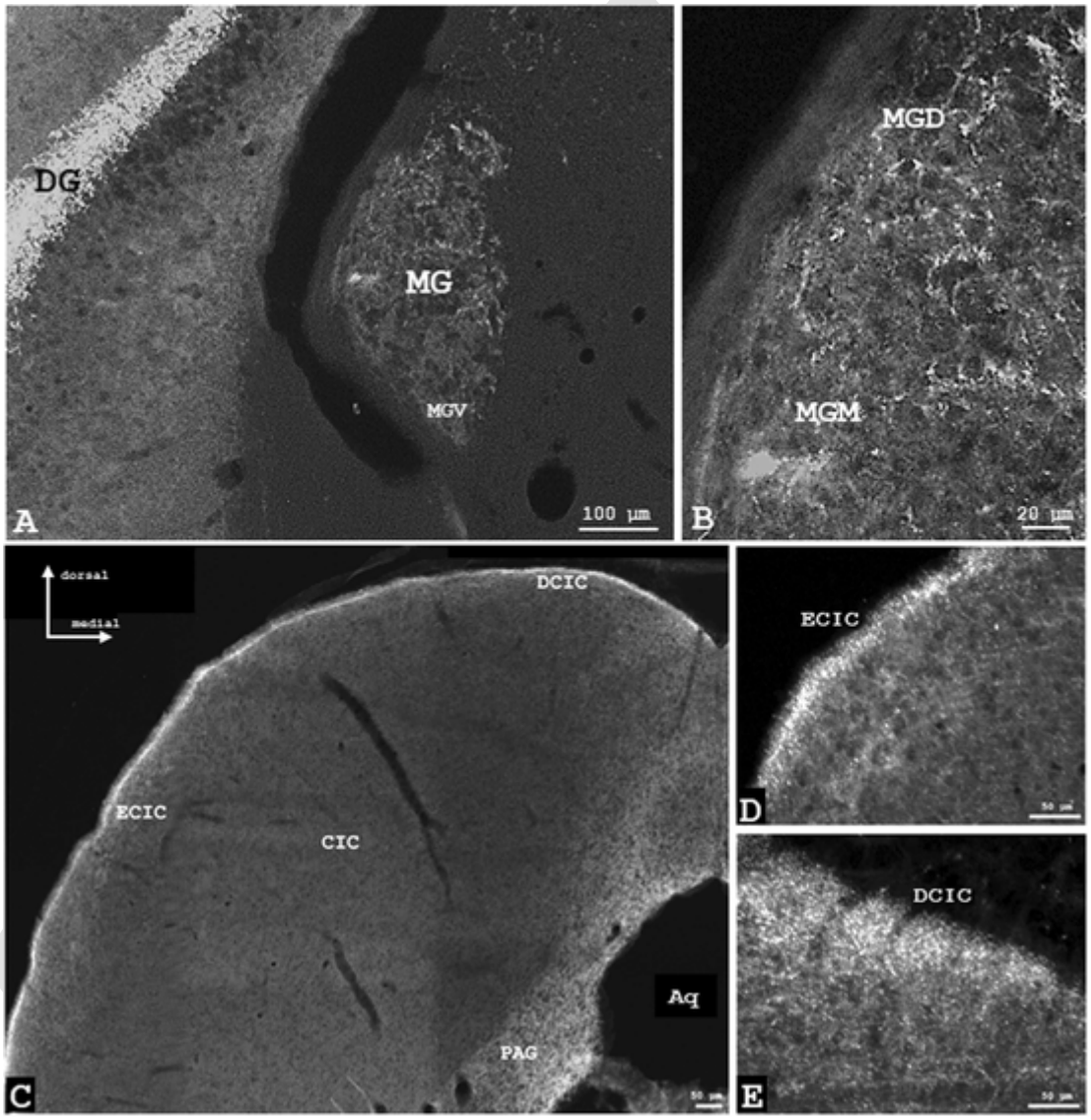

Fig. 2. Synaptoporin distribution in the mouse medial geniculate body (MG) and inferior colliculus (IC). (A) The MG shows differential synaptoporin-immunoreactivity. (B) Enlargement demonstrates that synaptoporin-immunoreactivity is of higher density in the dorsal (MGD) and medial parts (MGM) compared to its ventral part (MGV). Note the typical strong staining of mossy fibers in the granule cell layer of the dentate gyrus (DG). (C-E) The IC shows only sparse signals including the central part (CIC), while external and dorsal cortices (ECIC and DCIC) exhibit higher synaptoporin densities. Note the relatively strong staining in the periaqueductal gray (PAG) surrounding the cerebral aqueduct (Aq) in C. Orientation as shown in C applies to all panels.

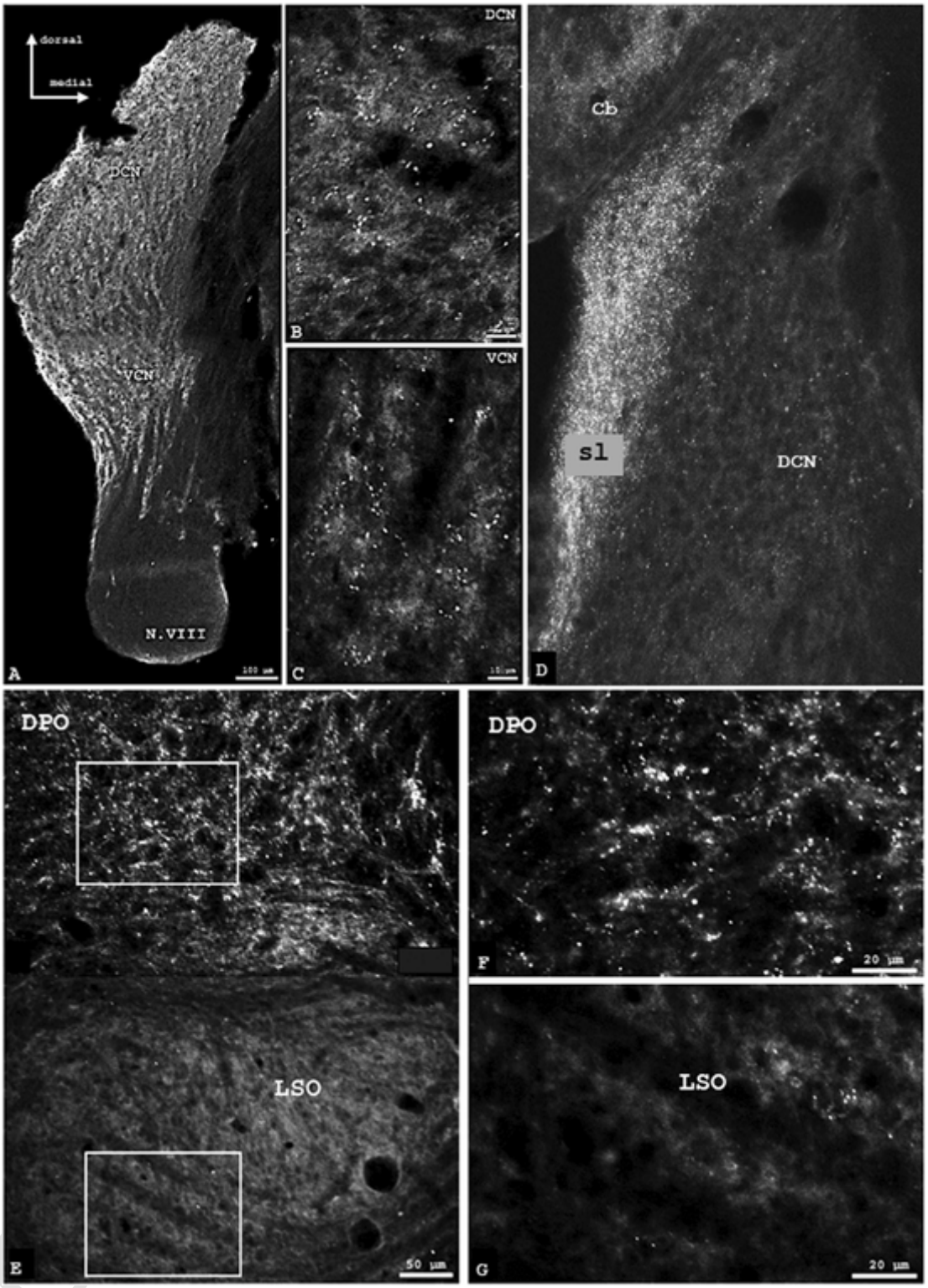

Fig. 3. Synaptoporin distribution in cochlear nucleus (A-D) and superior olivary complex (E-G) of the mouse. The overall staining is low in both, the dorsal (DCN in B) and ventral part (VCN in C). Dense labelling was observed in the laterally located superficial layer of the DCN (left DCN shown in D). CB cerebellum. (E) In the superior olivary complex, high density was present in the dorsal periolivary (DPO) nucleus, while scarce immunoreactivity was seen in the lateral superior olive (LSO). The higher magnifications (F, G) clearly demonstrate the difference in synaptoporin-immunofluorescence. Orientation as shown in A applies to all panels.

The cochlear nuclei (Fig. 1 D) exhibited relatively scarce immunoreactive labelling, which was often arranged in conspicuous circles of approximately 10 µm in diameter (Fig. 3 A–C). High staining density was seen in the superficial layer of the dorsal cochlear nucleus (Fig. 3 D).

Remarkable differences within one region were also observed in the superior olivary complex (Fig. 1 E). Its principal nuclei (lateral, medial and superior olive, medial nucleus of the trapezoid body) showed weak densities or were even devoid of synaptoporin (LSO shown in Fig. 3 EG). In contrast, the periolivary regions, in particular the dorsal perioli-

vary region (DPO), showed moderate to high immunofluorescence (Figs. 1 E, 3 F). The findings obtained with the custom-made guinea pig antibodies (see chapter 2.2) were consistent in all mice studied regardless of sex and strain. They were also very similar to findings in rat brain sections that were incubated with a commercial rabbit-raised synaptoporin antibody (see Section 2.5 and Table 1).

3.2. Identification of neurons contacted by synaptoporin puncta

The conspicuous staining pattern in SOC regions prompted us to conduct the second part of our study, in which we sought to identify and classify neurons in the SOC that are in contact with synaptoporin-positive puncta. To this end, double-immunofluorescence analyses were performed detecting synaptoporin in combination with different neurotransmitters, i.e. ChAT-, glutamate-, CGRP-, nNOS- and serotonin-immunofluorescence in murine brainstem sections. Typical results are provided in Figs. 4 and 5.

Punctate synaptoporin immunostaining was observed perisomatically in association with serotonergic, glutamatergic, and nitrergic neurons. Serotonin-positive neuronal somata were not found in the principal nuclei of the SOC but were present in the VPO and, to a lesser extent, in the DPO (Fig. 4 A). Synaptoporin-immunoreactive structures were seen throughout the SOC with an accumulation in periolivary regions. Densely spaced synaptoporin puncta were often observed near serotonin neurons in the ventral periolivary area (Fig. 4 BC).

The nitrergic cell group exhibited a distinct relationship with synaptoporin puncta. In particular, shell neurons immunoreactive to nNOS in the dorsal periolivary region (Fig. 4 D) were surrounded by synaptoporin-immunoreactive structures (Fig. 4 EF). Many of these neurons showed elongated somata and processes oriented parallel to the LSO. When neuronal processes were labeled by immunofluorescence, e.g., in nNOS-neurons (Fig. 4 F), synaptoporin puncta also covered these structures.

Glutamatergic somata were present throughout the SOC, in particular in the lateral limb of the LSO and in the ventral periolivary area (Fig. 5 A). In these regions, synaptoporin puncta were detected close to glutamate-positive cell bodies (Fig. 5 AB). In particular, concentrations of synaptoporin were present close to neurons in the VPO. An example is given in Fig. 5 C.

Synaptoporin puncta were not seen close to neurons immunoreactive to ChAT or CGRP, but were often present in the same regions, in many cases at neighboring non-immunoreactive neurons. Cholinergic neurons were distributed throughout the LSO, with higher density in the dorsal aspect of the lateral flank. Higher magnifications did not reveal synaptoporin-staining near ChAT-neurons. The same was true for CGRP-immunolabeled neurons which exhibited a similar distribution as ChAT-neurons. Cell bodies of both groups were relatively small, mainly spindle-shaped and aligned in a dorso-ventral direction.

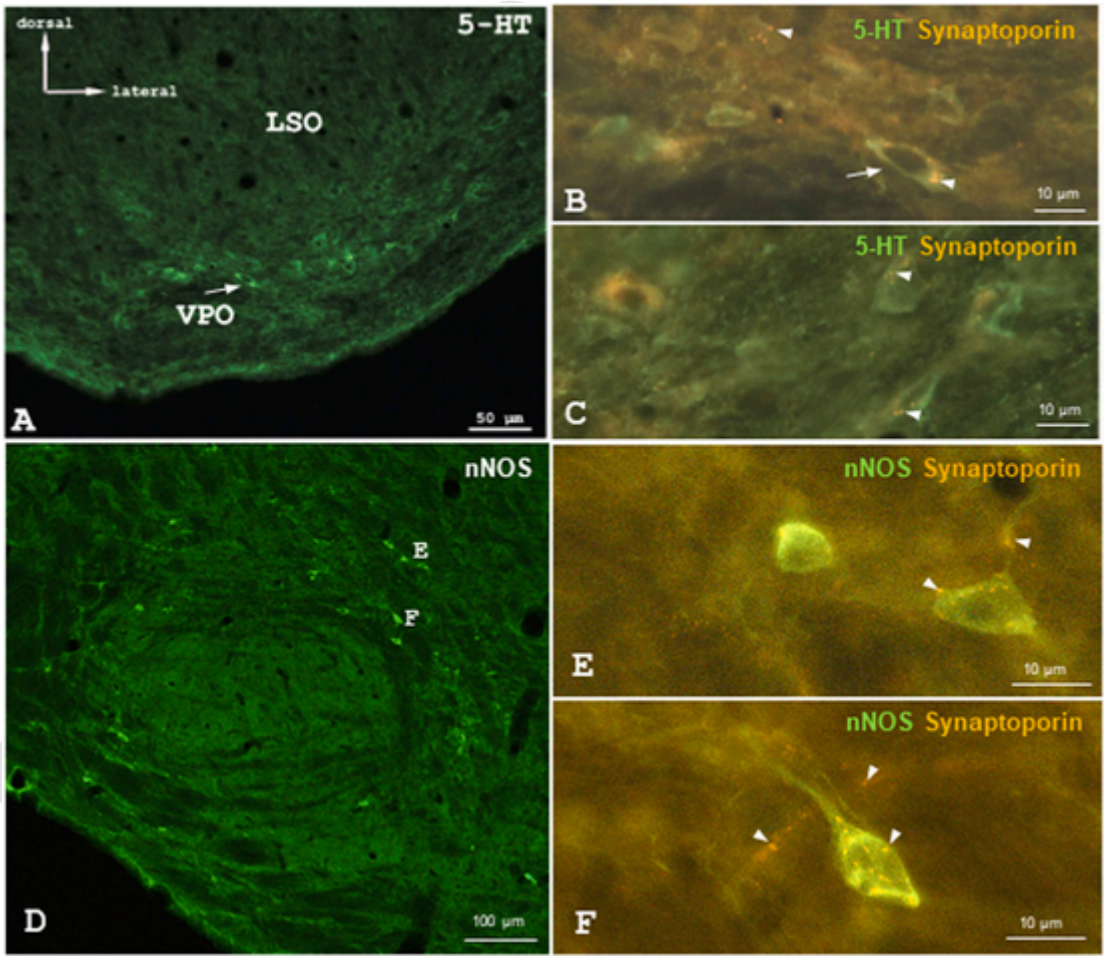

Fig. 4. Double-immunofluorescence in the mouse superior olivary complex (SOC) showing synaptoporin and serotonin or neuronal nitric oxide-synthase. (A) Distribution of serotonergic (5-HT) neurons in the LSO. (B,C) Higher magnification of the VPO region depicting high level of colocalization of synaptoporin puncta (white arrowheads) and serotonin immunoreactivity. The same neuron is marked by arrows in A and B. Note that synaptoporin density is higher in DPO and VPO compared to the LSO. (D) Location of nitrergic shell-neurons in the rostral SOC. Neurons marked with E and F are shown in higher magnification in the respective panels (E,F) in dual channel imaging of nNOS and synaptoporin (marked by white arrowheads). Orientation as shown in A applies to all panels.

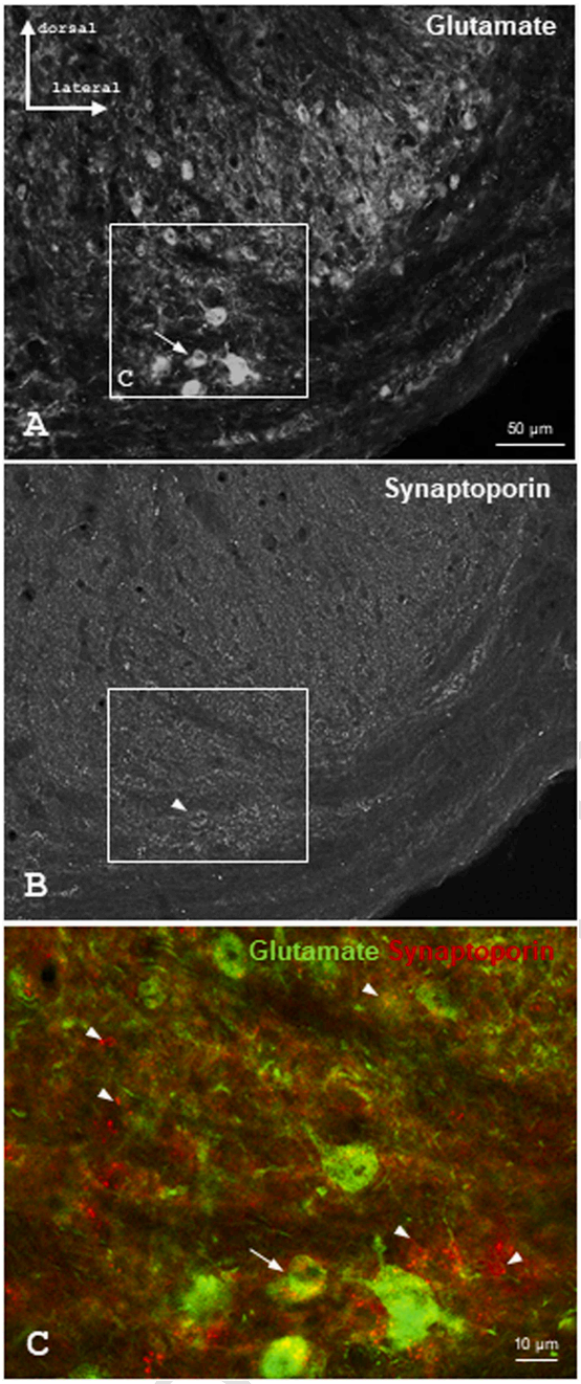

Fig. 5. Location in LSO and ventral periolivary area of glutamate-immunoreactive neurons (A) and (B) synaptoporin in the same section. (C) Dual channel image recording of boxed area in AB in higher magnification shows dense synaptoporin puncta at glutamate neurons in the VPO. The same neuron is marked by arrows in A and C, and the respective synaptoporin-puncta in B with an arrowhead. Orientation as shown in A applies to all panels.

3.3. Neuronal tracing and synaptoporin/PTH2 localization

The third part of our study, conducted in rats, dealt with the possible source of superior olivary synaptoporin-neurites from the medial paralemniscal nucleus (MPL), which is known as a main expression site of the protein PTH2 (Dobolyi et al., 2003b). Since the MPL is thought to contribute to non-auditory input to the SOC (Dobolyi et al., 2003b), we sought to investigate the MPL-SOC connection. We injected the anterograde neuronal tracer Pha-L into the MPL and studied its distribution in the SOC. We also compared the tracing pattern with the distribution of PTH2, and investigated both immunoreactivities with respect to synaptoporin.

The MPL exhibited high levels of PTH2 immunofluorescence (Fig. 6 A). The higher magnification showed that neuronal somata, fibers and punctate structures were labeled (Fig. 6 B). In contrast, the synaptoporin antibody labelled only puncta in high density in the MPL (Fig. 6 C).

Upon injection and anterograde neuronal tracing, many Pha-L-immunofluorescent fibers and puncta were observed in the ipsilateral dorsal periolivary region (Fig. 6 D). A similar distribution was found for synaptoporin (Fig. 6 E), i.e., a clear limitation to the DPO leaving out the LSO (Fig. 6 D–F). The higher magnification (Fig. 6 G) revealed no apparent colocalization of Pha-L and synaptoporin in the DPO. LSM imaging (Fig. 6 H) demonstrated immunolabeled synaptoporin spots in juxtaposition to Pha-L positive fibers.

When tracer injections into the MPL included neighboring structures, the tracing pattern did not differ significantly, as long as the MPL was included.

Neuronal tracing combined with PTH2-immunolabeling showed both substances in the same structures in many instances (Fig. 7 A-E). The overview in Fig. 7 AB and higher magnification in Fig. 7 CD illustrate that the respective immunoreactivities codistribute. LSM imaging further corroborated that fibers labeled by Pha-L injection into the MPL often colocalized with PTH2-immunolabeling (Fig. 7 E).

When synaptoporin and PTH2 were combined in double-immunofluorescence incubations, findings were principally identical to those obtained with synaptoporin and Pha-L, i.e., colocalization was very rare while juxtaposition was common (Fig. 7 F).

4. Discussion

4.1. Synaptoporin distribution

Using immunohistochemistry, we investigated the distribution of the vesicle protein synaptoporin in putative synaptic terminals and the corresponding postsynaptic target neurons in the subcortical auditory system. By combining immunostaining with neuronal tracing we searched for the neuronal somata corresponding to the synaptoporin-positive terminals.

Our findings on differential synaptoporin expression are in line with and extend previous reports, which detected synaptoporin immunoreactivity in hippocampus, cerebellum, cerebral cortex, dorsal root ganglia (DRG), spinal cord, olfactory bulb, and the superior colliculus (Bergmann et al., 1993; Chung et al., 2019; Fykse et al., 1993; Grabs et al., 1994; Knaus et al., 1990; Marquèze-Pouey et al., 1991; Sun et al., 2006). In our study, as in previous studies, the synaptoporin antibodies exclusively labeled punctate structures, the morphological identity of which was below the microscopical resolution limit. Since synaptoporin is a synaptic vesicle protein, the respective immunoreactivity most likely represents presynaptic terminals. This was substantiated by electron microscopy in rats (Singec et al., 2002) using the same antibody as in the present study, obtained commercially from Synaptic Systems (see Table 1). Of note, our present light-microscopical results match well with those described by Singec and co-workers (2002), as was the case with our mouse results obtained with the custom-made antibody with those obtained presently in rats with the Synaptic Systems-antibody.

We concentrated on synaptoporin distribution in the auditory system, which has not received much attention in previous studies, and its possible functional implications. We observed remarkable differences in synaptoporin staining density in subcortical auditory structures. Interestingly, synaptoporin was barely detectable in brain regions of the canonical auditory pathway, i.e., in the core of the cochlear nucleus,

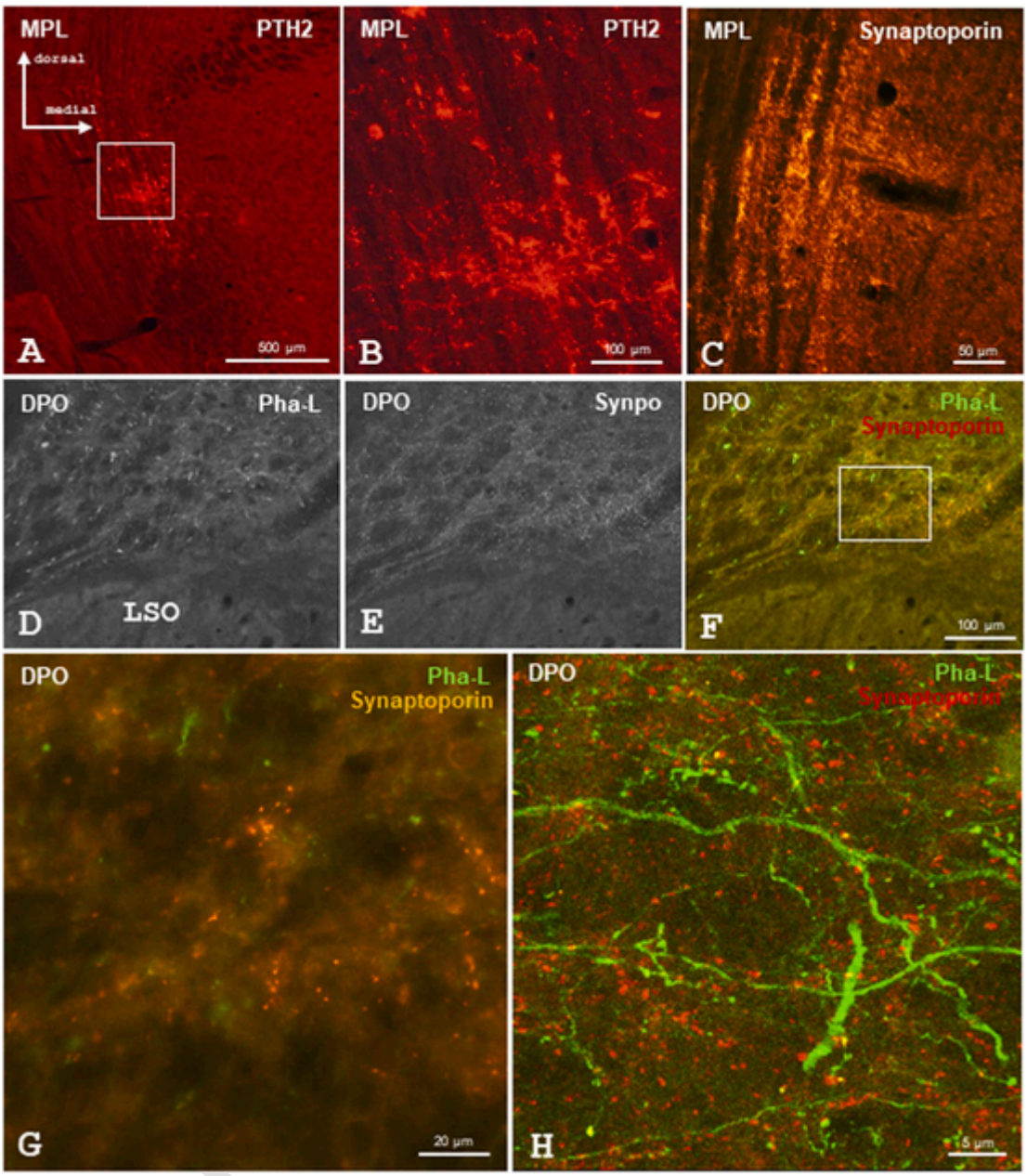

Fig. 6. Immunofluorescence in the rat brain. (A-C) depicts the medial paralemniscal nucleus (MPL) with (A) PTH2-immunoreactive neuronal cell bodies and fibers. Boxed area is shown in higher magnification in (B). High synaptoporin density in a corresponding section from mouse brain (C). Panels D-G demonstrate the dorsal periolivary area, just dorsal to the LSO, upon Pha-L tracer injection into the MPL and anterograde neuronal transport. (D) stained for Pha-L, (E) same section labeled for synaptoporin, and (F) dual band filter set image of both signals. The boxed area in (F) is given in higher magnification in (G) revealing no colocalization of tracer (green) and synaptoporin (red). (H) LSM image of a corresponding section also demonstrating no evident colocalization, but that synaptoporin-puncta (red) were often found close to Pha-L fibers (green). Orientation as shown in A applies to all panels.

LSO, the nuclei of the lateral lemniscus and the central part of the inferior colliculus.

To process pure acoustic information such as frequency and localization, the neurons of the canonical auditory pathway are primarily innervated by axons originating from other upstream or downstream auditory centers. We detected strong synaptoporin immunolabeling in the superficial layers of inferior colliculus, in the dorsal cochlear nucleus and periolivary regions as well as in the medial paralemniscal nucleus and periaqueductal grey. These structures are not tonotopically organized (Clopton et al., 1974). They are known as targets of multimodal projections to the auditory system. Fitting to the observation that classical auditory system structures are often surrounded by components receiving non-auditory input, our present results suggest that synaptoporin is expressed mainly in auditory components that constitute an interface between the auditory system and across modalities, i.e., in terminals of extra-auditory origin.

The high level of synaptoporin expression in the superficial layer of the dorsal cochlear nucleus is of particular interest. This region, containing the granule layer, receives input from various nuclei such as cuneate, trigeminal, lateral reticular and inferior olive (cf. Ryugo et al., 2003), and thus from regions mediating cutaneous, proprioceptive, and motor functions. Likewise, multimodal connections are present in other regions such as the cortical regions of the IC and parts of the medial geniculate body, which distinctly stained for synaptoporin in the present study. Previous studies using neural imaging showed that listening to music activates not only auditory regions of the brain but also those

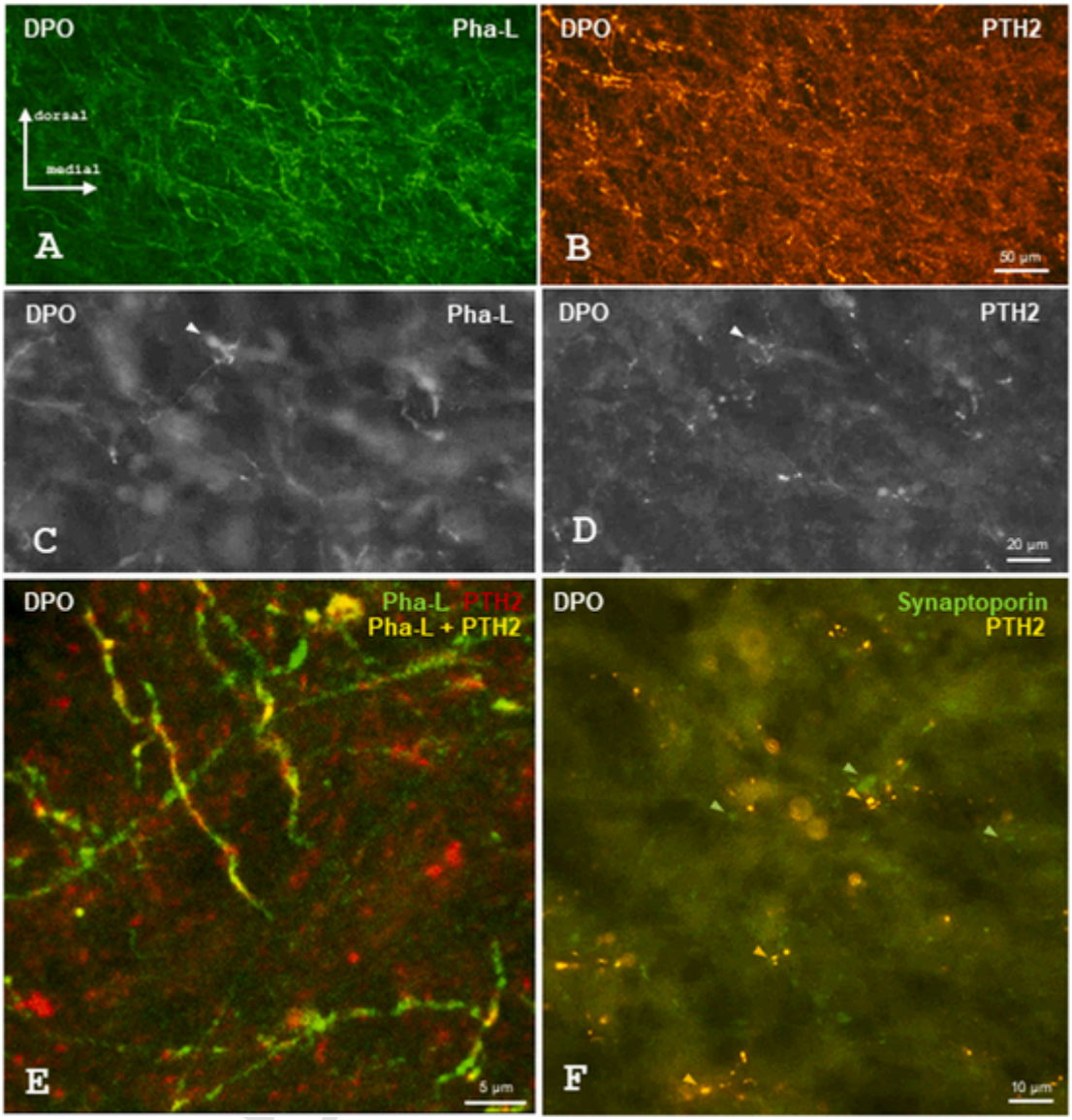

Fig. 7. Immunofluorescence microscopy in the rat brain. (A-E) depicts the dorsal periolivary area (DPO) with combined Pha-L and PTH2 immunofluorescences. (A) Pha-L in the DPO and (B) PTH2-immunoreactivity in the same section. Higher magnifications from this section are given in (C) and (D) demonstrating Pha-L and PTH2 fibers and puncta with similar distribution and partial colocalization (exemplarily marked by white arrowheads). (E) LSM image demonstrating clear partial coexistence (yellow) of Pha-L (green) and PTH2 (red). (F) dual band filter set image of synaptoporin (green, marked by green arrowheads) and PTH2 (red-yellow, marked by arrowheads) showing no colocalization but close neighborhood in some instances. Orientation as shown in A applies to all panels.

involved in motor, visual and emotional processing (cf. Blood and Zatorre, 2001; Limb, 2006).

Not much information is available about synaptoporin´s functional role. Interestingly, it was suggested that synaptoporin-enriched mossy fiber terminals at CA3 pyramidal neurons are involved in epilepsy hyperexcitability (André et al., 2018). These synapses may work as a gain control instance permitting homeostatic adjustment, and the associated synaptic plasticity may require synaptoporin (Lee et al., 2013).

Whether a similar role applies to synaptoporin in auditory regions is not known. Our data, however, suggest its involvement in regulatory processes also in the SOC´s periolivary regions, which are interconnected to other nuclei of the SOC and probably are involved in cochlear feedback mechanisms (Spangler et al., 1985). Interestingly, synaptoporin puncta were often arranged in circles of 10–20 µm diameter around unlabeled structures, suggesting synaptic contacts with neurons in the respective regions. Similar arrangements were observed previously by Singec et al. (2002) in the hippocampus. Taken together, our observations suggest a complex and region-specific synaptoporin expression in the auditory system.

4.2. Identification of neurons targeted by synaptoporin-puncta in the superior olivary complex

An open question was which types of neurons are likely to be affected by synaptoporin-containing synapses. In the second part of our study, we therefore sought to characterize the synaptoporin-targeted neurons by means of double-immunofluorescence. As region of interest we selected the SOC, an important auditory relay center that plays a prominent role in mammalian sound localization (Grothe et al., 2010). It sends efferents to a variety of auditory structures such as the inferior colliculus, and provides the olivocochlear efferent innervation that regulates hair cell electromotility, sound amplification and auditory transmission by afferent fibers. Involved are the lateral olivocochlear (LOC) system providing efferent regulation of inner hair cell (IHC) afferents stemming from type I spiral ganglion cells, and the medial OC (MOC)

efferents that synapse directly at outer hair cells (OHC). We selected five substances belonging to different functional systems, i.e. ChAT, CGRP, glutamate, nNOS, and serotonin. All were known to be present in the SOC (Bartolomé and Gil-Loyzaga, 2005; Lu et al., 1987; Moore and Moore, 1987; Reuss, 1998; Safieddine et al., 1997).

Neurons expressing ChAT or CGRP, clearly identified as transmitters within the OC systems (cf. Raphael and Altschuler, 2003), were found in the present study to not be contacted by synaptoporin puncta. These substances, however, were mostly observed in intrinsic LOC and in MOC neurons (cf. Guinan, 2018), while synaptoporin was found predominantly in the shell regions. In particular, punctate synaptoporin immunostaining was observed perisomatically at serotonergic, glutamatergic, and nitrergic neurons, suggesting synaptic contacts with these cells.

Serotonergic neurons and synaptoporin puncta were located in close vicinity in the ventral periolivary region. They belong to the group of shell neurons in rostral and dorsal SOC regions, and may provide the serotonergic innervation of the cochlea (cf. Bartolomé and Gil-Loyzaga, 2005). These neurons are probably not involved in pure tone transduction but, for example, in alertness and attention mechanisms (cf. Bartolomé and Gil-Loyzaga, 2005). Shell neurons such as the serotonergic cells, as observed in the present study, project to IHC as part of the LOC system but may reach OHC as well (Gil-Loyzaga et al., 2000). Serotonin receptors, which may modulate the transduction of the mechanosensory signal, were found in the organ of Corti and in other cochlear structures (Oh et al., 1999).

Glutamatergic neurons, located in the LSO and in periolivary regions, appear to be contacted by synaptoporin-positive puncta. They are located mainly in the lateral (low frequency) limb of the LSO and in the ventral periolivary area as described previously for rat and monkey (Ito et al., 2011; Wynne et al., 1995). These excitatory neurons provide ascending projection to the IC and also belong to the olivocochlear group of neurons (Fex and Altschuler, 1984).

The third group of neurons that apparently received synaptoporin-mediated contacts are nitrergic SOC cells. They were identified as expressing neuronal nitric oxide synthase (nNOS), the enzyme responsible for nitric oxide (NO) synthesis (Fessenden et al., 1999; Reuss, 1998). In rats, they encompass neurons projecting to cochlea and IC (Riemann and Reuss, 1999; Schaeffer et al., 2003). Localization and morphology of the nitrergic neurons identified characterize them as shell-neurons belonging to the lateral olivocochlear system (Sánchez-González et al., 2003) indicating a very restricted localization in mouse compared to rat and guinea pig (Riemann and Reuss, 1999). The gaseous substance NO activates cGMP-production and may modulate cell metabolism and neurotransmitter release. These effects may as well occur at the level of the lower auditory brainstem, since NO-mediated suppression of transmission in SPN was described (Yassin et al., 2014). Nitric oxide may inhibit the ATP-mediated Ca^{2+} influx at IHC in a cochlear feedback mechanism (Shen et al., 2005). It is so far open what the projection pattern and function of synaptoporin-controlled NO-producing neurons are. In rats, ascending and efferent nitrergic neuronal groups represent only a fraction of the total number of these neurons in the SOC.

The latter specification applies, however, to all neuronal groups described here that supposedly do or do not receive synaptoporin-involving contacts. It is not easily recognizable which intrinsic transmitter or projection pattern qualifies for synaptoporin-involving putative innervation. Glutamatergic neurons with collicular and/or olivocochlear projection pattern and serotonergic neurons that do not project to the cochlea are clearly contacted. Cholinergic and CGRP-ergic neurons, predominantly belonging to LOC and MOC systems, are not contacted by synaptoporin. Further studies using identification of neuronal groups by retrograde neuronal tracing, combined with immunofluorescent detection of transmitter candidates and of synaptoporin, will answer this question.

4.3. Possible sources of synaptoporin in the superior olivary complex

Assuming that synaptoporin marks extra-auditory influence on auditory processing, it is of interest where these projections may arise. Neural processing of auditory stimuli incorporates information on many brain functions such as vision, balance, somatic sensation, learning, memory, and emotional state. This requires a stable but plastic transmission system probably involving differentially regulated synaptic mechanisms. Synaptoporin may play a special role independent from other members of the physin family (Hübner et al., 2002), as revealed by their different expression patterns. It is conceivable that synaptic vesicles in different pathways may vary in their molecular composition.

Notably, synaptoporin-positive neuronal perikarya were not observed in previous (Fykse et al., 1993; Grabs et al., 1994; Knaus et al., 1990; Marquèze-Pouey et al., 1991) or the present study, and there is thus no information available where synaptoporin-expressing cell bodies providing projections to the DPO are located. On the other hand, a considerable number of sites are known to connect to the DPO. For example, glutamatergic layer V pyramidal cells in primary and secondary auditory cortices project to periolivary regions (as well as to LSO and paralemniscal regions) (Brown et al., 2013; Doucet et al., 2002; Feliciano et al., 1995). Cholinergic input to DPO originates in pontomesencephalic tegmentum and reticular formation (Beebe et al., 2021), and serotoninergic fibers of unknown source(s) are densely accumulated in periolivary regions where shell neurons are located (Steinbusch, 1981; Thompson and Schofield, 2000).

Although it was open which site(s) provide the DPO projection involving synaptoporin, a major candidate was the medial paralemniscal nucleus (MPL). It was shown to project to those auditory regions rich in synaptoporin immunofluorescence, e.g. the medial geniculate body, the external cortex of the inferior colliculus and the periolivary nuclei (Dobolyi et al., 2003a). Furthermore, we observed that synaptoporin is concentrated in the periaqueductal grey and in deep layers of the superior colliculus, which are also targeted by efferent projections of the MPL. It may be assumed that terminals originating from the MPL contain synaptoporin as a vesicle protein. The MPL is massively interconnected with those auditory regions where we found synaptoporin expression (Varga et al., 2008), and itself exhibits the highest density of synaptoporin staining. In particular, MPL neurons were suggested to participate in mediating audiogenic stress responses (Palkovits et al., 2004).

The DPO is involved in the integration of multisensory information, and receives extra-auditory input, partly from the medial paralemniscal nucleus (MPL). Most neurons of this nucleus express parathyroid hormone 2 (PTH2), which was first described as tuberoinfundibular peptide of 39 residues (TIP39; (Dobolyi et al., 2002; Palkovits et al., 2004). It is involved in the regulation of many neural functions such as nociception, thermoregulation, reproduction, and social interactions. In the auditory system, PTH2 was found, inter alia, in fibers in medial MGB, PAG, IC and SOC where also fibers and/or cell bodies were seen that express the PTH2-receptor. It is believed that PTH2 may modulate information such as noise-induced stress responses (cf. Dobolyi et al., 2010; Keller et al., 2022b). Taken together, a large body of evidence suggests that the MPL, using PTH2 as transmitter, presumably innervates the periolivary regions of the SOC.

4.4. MLP projections to DPO

The third part of our study, conducted in rats, dealt with the possible source of superior olivary synaptoporin from the medial paralemniscal nucleus, which stands out by a high density of synaptoporin, and is thought to contribute to non-auditory input to the SOC (Dobolyi et al., 2003b). We therefore injected the anterograde neuronal tracer PhaL into the MPL and studied its distribution in the SOC. We also com-

pared this with the distribution of PTH2 in this region, and investigated both immunoreactivities with respect to synaptoporin.

The most clear-cut result was the coexistence of PTH2 and the neuronal tracer Pha-L after stereotactic injection into the MPL. Many fibers and puncta, just dorsal to and particularly in the DPO, exhibited both immunofluorescences simultaneously. Of note, when tracer applications included neighboring structures (see Fig. 1 B), the appearance of Pha-L immunoreactivity in the SOC did not differ from the pattern found upon MPL-restricted injections. This may be in part attributed to the fact that fibers of passage do not take up Pha-L (cf. (Gerfen and Sawchenko, 2016). In addition, neurons of the laterally located nuclei of the lateral lemniscus, in particular of its ventral group, project to the IC (cf. (Malmierca, 2015) but not to the SOC. Furthermore, neurons of the medially located oral part of the pontine reticular nucleus innervate the spinal cord but are not among those projecting to the SOC region (Liang et al., 2015).

Our data demonstrate that the MPL is a major source of projection to the DPO and that PTH2 is involved as transmitter substance. Our findings fit well to the observation that PTH2 in the SOC disappears upon lesion of the MPL (Dobolyi et al., 2003a).

Pha-L and synaptoporin showed a similar distribution in the SOC, with a clear restriction to the dorsal DPO and exclusion of the LSO. It was also apparent that structures labeled by the neuronal tracer did not contain synaptoporin. Epifluorescence and laser-scanning confocal microscopy did not provide evidence that both immunoreactivities codistribute, suggesting that the MPL is not the source of synaptoporin in the SOC.

The observation of some rare PTH2/synaptoporin colocalizations in the DPO may suggest that a minor portion of synaptoporin stem from other PTH2-expressing sites yet to be determined. It was striking, however, that synaptoporin and Pha-L or PTH2 were often localized in close vicinity. These results suggest that both, synaptic contacts of synaptoporin-terminals of predominantly unknown origin and PTH2-input from the MPL interact in the DPO.

4.5. Technical considerations

Although the present study sought to explore the structures in a qualitative manner, some aspects should be pointed out that may have influenced the results. First, in the present study we did not treat animals with the unspecific axonal transport blocker colchicine. This may have led to an underestimation of the true number of neurons that produce a substance under investigation in cases where the amount is low. Second, the injection of Pha-L into the MPL and the subsequent transport may influence synaptoporin and or PTH2 expression in the MPL and may affect axonal transport mechanism to the SOC. Third, antigen retrieval and tyramide amplification procedures may have influenced the appearance of respective immunoreactivities.

4.6. Conclusion

Our data demonstrate that the synaptic vesicle protein synaptoporin is present in various brain regions involved in providing or processing non-auditory input to auditory structures in mice and rats. One of these is the periolivary area of the auditory brainstem, which exhibited a high density of synaptoporin immunostaining. The origin of this projection, which is associated with serotonergic, glutamatergic and nitrergic neurons, remains unknown. A second pathway, originating in the MPL and using PTH2 as a transmitter, is not identical to the projection characterized by synaptoporin. However, there is ample morphological evidence that these inputs may interact locally in processing multimodal information in the lower auditory brainstem. Our findings shed new light on the distribution and function of synaptoporin-containing pathways. Finally, it will be desirable to answer the following questions. Where do the synaptoporin-positive structures in the DPO originate? Would a lesion of the MPL influence their distribution? Would audiogenic stress affect synaptoporin in the DPO?

CRediT authorship contribution statement

SR: study concept and design; study supervision; analysis and interpretation of data, draft manuscript for intellectual content; critical revision of manuscript for intellectual content; DL, JBB, JvR,: acquisition of data; analysis and interpretation of data, critical revision of manuscript for intellectual content; SM, UDK: acquisition and analysis of data; TU, REL: generation and validation of custom-made antibodies, critical revision of manuscript for intellectual content.

Conflict of Interest

All authors declare that the research was conducted in the absence of any commercial or financial relationships that could be construed as a potential conflict of interest.

Acknowledgements

The authors thank Ms. Ursula Wilhelm for valuable help with characterization of the custom-made synaptoporin-antibody. The neuroanatomical lab work was conducted while SR was Head of the Functional Neuroanatomy Group at the Department of Anatomy and Cell Biology, University Medical Center, Mainz. The manuscript contains data from the MD theses of D.L, J.B.-B. and J.v.R. Our studies of the auditory system were funded by Röttger-Stiftung (Bad Vilbel, Germany), Hoffmann-Klose-Stiftung (Kronberg, Germany), and Schleicher-Stiftung (Baden-Baden, Germany). None of the sponsors had any influence in the study design, the collection, analysis and interpretation of data, the writing of the manuscript and in the decision to submit the article for publication.

References

André, E.A., Forcelli, P.A., Pak, D.T., 2018. What goes up must come down: homeostatic synaptic plasticity strategies in neurological disease. Future Neurol. 13, 13–21. https://doi.org/10.2217/fnl-2017-0028.

Bartolomé, M.V., Gil-Loyzaga, P., 2005. Serotonergic innervation of the inner ear: is it involved in the general physiological control of the auditory receptor? Int Tinnitus J. 11, 119–125.

Beebe, N.L., Zhang, C., Burger, R.M., Schofield, B.R., 2021. Multiple sources of cholinergic input to the superior olivary complex. Front. Neural Circuits 15, 715369. https://doi.org/10.3389/fncir.2021.715369.

Bergmann, M., Schuster, T., Grabs, D., Marquèze-Pouey, B., Betz, H., Traurig, H., Mayerhofer, A., Gratzl, M., 1993. Synaptophysin and synaptoporin expression in the developing rat olfactory system. Dev. Brain Res. 74, 235–244. https://doi.org/10.1016/0165-3806(93)90009-y.

Betz, H., 1990. Homology and analogy in transmembrane channel design: lessons from synaptic membrane proteins. Biochemistry 29, 3591–3599. https://doi.org/10.1021/bi00467a001.

Blood, A.J., Zatorre, R.J., 2001. Intensely pleasurable responses to music correlate with activity in brain regions implicated in reward and emotion. Proc. Natl. Acad. Sci. USA 98, 11818–11823. https://doi.org/10.1073/pnas.191355898.

Bobrow, M.N., Litt, G.J., Shaughnessy, K.J., Mayer, P.C., Conlon, J., 1992. The use of catalyzed reporter deposition as a means of signal amplification in a variety of formats. J. Immunol. Methods 150, 145–149. https://doi.org/10.1016/0022-1759(92)90073-3.

Brown, M.C., Mukerji, S., Drottar, M., Windsor, A.M., Lee, D.J., 2013. Identification of inputs to olivocochlear neurons using transneuronal labeling with pseudorabies virus (PRV). J. Assoc. Res. Otolaryngol.: JARO 14, 703–717. https://doi.org/10.1007/s10162-013-0400-5.

Chung, J., Franklin, J.F., Lee, H.J., 2019. Central expression of synaptophysin and synaptoporin in nociceptive afferent subtypes in the dorsal horn. Sci. Rep. 9, 4273. https://doi.org/10.1038/s41598-019-40967-y.

Clopton, B.M., Winfield, J.A., Flammino, F.J., 1974. Tonotopic organization: review and analysis. Brain Res. 76, 1–20. . https://doi.org/0006-8993(74)90509-5 [pii].

Dobolyi, A., Palkovits, M., Bodnar, I., Usdin, T.B., 2003a. Neurons containing tuberoinfundibular peptide of 39 residues project to limbic, endocrine, auditory and spinal areas in rat. Neuroscience 122, 1093–1105. . https://doi.org/S0306452203006717 [pii].

Dobolyi, A., Palkovits, M., Usdin, T.B., 2003b. Expression and distribution of tuberoinfundibular peptide of 39 residues in the rat central nervous system. J. Comp. Neurol. 455, 547–566. https://doi.org/10.1002/cne.10515.

Dobolyi, A., Palkovits, M., Usdin, T.B., 2010. The TIP39-PTH2 receptor system: unique peptidergic cell groups in the brainstem and their interactions with central regulatory mechanisms. Prog. Neurobiol. 90, 29–59. https://doi.org/10.1016/j.pneurobio.2009.10.017.

Dobolyi, A., Ueda, H., Uchida, H., Palkovits, M., Usdin, T.B., 2002. Anatomical and physiological evidence for involvement of tuberoinfundibular peptide of 39 residues in nociception. Proc. Natl. Acad. Sci. USA 99, 1651–1656. https://doi.org/10.1073/pnas.042416199.

Doucet, J.R., Rose, L., Ryugo, D.K., 2002. The cellular origin of corticofugal projections to the superior olivary complex in the rat. Brain Res. 925, 28–41. https://doi.org/10.1016/s0006-8993(01)03248-6.

Feliciano, M., Saldaña, E., Mugnaini, E., 1995. Direct projections from the rat primary auditory neocortex to nucleus sagulum, paralemniscal regions, superior olivary complex and cochlear nuclei. Audit. Neurosci. 1, 287–308.

Fessenden, J.D., Altschuler, R.A., Seasholtz, A.F., Schacht, J., 1999. Nitric oxide/cyclic guanosine monophosphate pathway in the peripheral and central auditory system of the rat. J. Comp. Neurol. 404, 52–63. https://doi.org/10.1002/(SICI)1096-9861(19990201)404:1<52::AID-CNE4>3.0.CO;2-W.

Fex, J., Altschuler, R.A., 1984. Glutamic acid decarboxylase immunoreactivity of olivocochlear neurons in the organ of Corti of guinea pig and rat. Hear. Res. 15, 123–131. https://doi.org/10.1016/0378-5955(84)90043-1.

Fykse, E.M., Takei, K., Walch-Solimena, C., Geppert, M., Jahn, R., De Camilli, P., Südhof, T.C., 1993. Relative properties and localizations of synaptic vesicle protein isoforms: the case of the synaptophysins. J. Neurosci. 13, 4997–5007. https://doi.org/10.1523/JNEUROSCI.13-11-04997.1993.

Gerfen, C.R., Sawchenko, P.E., 1984. An anterograde neuroanatomical tracing method that shows the detailed morphology of neurons, their axons and terminals: immunohistochemical localization of an axonally transported plant lectin, Phaseolus vulgaris leucoagglutinin (PHA-L). Brain Res. 290, 219–238. https://doi.org/10.1016/0006-8993(84)90940-5.

Gerfen, C.R., Sawchenko, P.E., 2016. An anterograde neuroanatomical tracing method that shows the detailed morphology of neurons, their axons and terminals: immunohistochemical localization of an axonally transported plant lectin, Phaseolus vulgaris-leucoagglutinin (PHA-L). Brain Res. 1645, 42–45. https://doi.org/10.1016/j.brainres.2015.12.040.

Gil-Loyzaga, P., Bartolomé, V., Vicente-Torres, A., Carricondo, F., 2000. Serotonergic innervation of the organ of Corti. Acta oto-Laryngol. 120, 128–132. https://doi.org/10.1080/000164800750000757.

Grabs, D., Bergmann, M., Schuster, T., Fox, P.A., Brich, M., Gratz, M., 1994. Differential expression of synaptophysin and synaptoporin during pre- and postnatal development of the rat hippocampal network. Eur. J. Neurosci. 6, 1765–1771. https://doi.org/10.1111/j.1460-9568.1994.tb00569.x.

Grothe, B., Pecka, M., McAlpine, D., 2010. Mechanisms of sound localization in mammals. Physiol. Rev. 90, 983–1012. https://doi.org/10.1152/physrev.00026.2009.

Guinan, Jr, J.J., 2018. Olivocochlear efferents: their action, effects, measurement and uses, and the impact of the new conception of cochlear mechanical responses. Hear. Res. 362, 38–47. https://doi.org/10.1016/j.heares.2017.12.012.

Hübner, K., Windoffer, R., Hutter, H., Leube, R.E., 2002. Tetraspan vesicle membrane proteins: synthesis, subcellular localization, and functional properties. Int. Rev. Cytol. 214, 103–159. https://doi.org/10.1016/s0074-7696(02)14004-6.

Ito, T., Bishop, D.C., Oliver, D.L., 2011. Expression of glutamate and inhibitory amino acid vesicular transporters in the rodent auditory brainstem. J. Comp. Neurol. 519, 316–340. https://doi.org/10.1002/cne.22521.

Liang, H., Watson, C., Paxinos, G., 2015. Projections from the oral pontine reticular nucleus to the spinal cord of the mouse. Neurosci. Lett. 584, 113–118. https://doi.org/10.1016/j.neulet.2014.10.025.

Keller, D., Láng, T., Cservenák, M., Puska, G., Barna, J., Csillag, V., Farkas, I., Zelena, D., Dóra, F., Küppers, S., Barteczko, L., Usdin, T.B., Palkovits, M., Hasan, M.T., Grinevich, V., Dobolyi, A., 2022a. A thalamo-preoptic pathway promotes social grooming in rodents. Curr. Biol.: CB 32 (4593–4606), e4598. https://doi.org/10.1016/j.cub.2022.08.062.

Keller, D., Tsuda, M.C., Usdin, T.B., Dobolyi, A., 2022b. Behavioural actions of tuberoinfundibular peptide 39 (parathyroid hormone 2. J. Neuroendocrinol. e13130. https://doi.org/10.1111/jne.13130.

Knaus, P., Marquèze-Pouey, B., Scherer, H., Betz, H., 1990. Synaptoporin, a novel putative channel protein of synaptic vesicles. Neuron 5, 453–462. . https://doi.org/0896-6273(90)90084-S [pii].

Lee, K.J., Queenan, B.N., Rozeboom, A.M., Bellmore, R., Lim, S.T., Vicini, S., Pak, D.T., 2013. Mossy fiber-CA3 synapses mediate homeostatic plasticity in mature hippocampal neurons. Neuron 77, 99–114. https://doi.org/10.1016/j.neuron.2012.10.033.

Limb, C.J., 2006. Structural and functional neural correlates of music perception. Anat. Rec. Part A, Discov. Mol., Cell., Evolut. Biol. 288, 435–446. https://doi.org/10.1002/ar.a.20316.

Lu, S.M., Schweitzer, L., Cant, N.B., Dawbarn, D., 1987. Immunoreactivity to calcitonin gene-related peptide in the superior olivary complex and cochlea of cat and rat. Hear. Res. 31, 137–146. https://doi.org/10.1016/0378-5955(87)90119-5.

Malmierca, M.S., 2015. Auditory System. In: Paxinos, G. (Ed.), The Rat Nervous System. 4 ed., Academic Press, Amsterdam, pp. 863–946. https://doi.org/10.1016/B978-0-12-374245-2.00029-2.

Marquèze-Pouey, B., Wisden, W., Malosio, M.L., Betz, H., 1991. Differential expression of synaptophysin and synaptoporin mRNAs in the postnatal rat central nervous system. J. Neurosci. 11, 3388–3397. https://doi.org/10.1523/JNEUROSCI.11-11-03388.1991.

McLean, I.W., Nakane, P.K., 1974. Periodate-lysine-paraformaldehyde fixative. A new fixation for immunoelectron microscopy. J. Histochem Cytochem 22, 1077–1083. https://doi.org/10.1177/22.12.1077.

Moore, J.K., Moore, R.Y., 1987. Glutamic acid decarboxylase-like immunoreactivity in brainstem auditory nuclei of the rat. J. Comp. Neurol. 260, 157–174. https://doi.org/10.1002/cne.902600202.

Mulders, W.H., Robertson, D., 2001. Origin of the noradrenergic innervation of the superior olivary complex in the rat. J. Chem. Neuroanat. 21, 313–322. https://doi.org/10.1016/s0891-0618(01)00118-1.

Oh, C.K., Drescher, M.J., Hatfield, J.S., Drescher, D.G., 1999. Selective expression of serotonin receptor transcripts in the mammalian cochlea and its subdivisions. Brain Res. Mol. Brain Res. 70, 135–140. https://doi.org/10.1016/s0169-328x(99)00110-2.

Palkovits, M., Dobolyi, A., Helfferich, F., Usdin, T.B., 2004. Localization and chemical characterization of the audiogenic stress pathway. Ann. N. Y Acad. Sci. 1018, 16–24. https://doi.org/10.1196/annals.1296.002.

Palkovits, M., Helfferich, F., Dobolyi, A., Usdin, T.B., 2009. Acoustic stress activates tuberoinfundibular peptide of 39 residues neurons in the rat brain. Brain Struct. Funct. 214, 15–23. https://doi.org/10.1007/s00429-009-0233-5.

Paxinos, G., Franklin, K.B.J., 2013. The mouse brain in stereotaxic coordinates, fourth edition, 4th ed. Elsevier.

Paxinos, G., Watson, C., 2014. The rat brain in stereotaxic coordinates, 7 ed.,. Academic Press, San Diego.

Raphael, Y., Altschuler, R.A., 2003. Structure and innervation of the cochlea. Brain Res. Bull. 60, 397–422. https://doi.org/10.1016/s0361-9230(03)00047-9.

Reuss, S., 1998. Nitric oxide synthase in the auditory brain stem. Neuroreport 9, 3643–3646.

Reuss, S., 2021. Spinal relay neurons for central control of autonomic pathways in a photoperiodic rodent. J. Integr. Neurosci. 20, 561–571. https://doi.org/10.31083/j.jin2003060.

Reuss, S., Banica, O., Elgurt, M., Mitz, S., Disque-Kaiser, U., Riemann, R., Hill, M., Jaquish, D.V., Koehrn, F.J., Burmester, T., Hankeln, T., Woolf, N.K., 2016. Neuroglobin expression in the mammalian auditory system. Mol. Neurobiol. 53, 1461–1477. https://doi.org/10.1007/s12035-014-9082-1.

Reuss, S., Decker, K., 1997. Anterograde tracing of retinohypothalamic afferents with Fluoro-Gold. Brain Res. 745, 197–204. https://doi.org/10.1016/s0006-8993(96)01151-1.

Reuss, S., Disque-Kaiser, U., DeLiz, S., Ruffer, M., Riemann, R., 1999. Immunfluorescence study of neuropeptides in identified neurons of the rat auditory superior olivary complex. Cell Tissue Res 297, 13–21. https://doi.org/10.1007/s004410051329.

Reuss, S., Kühn, I., Windoffer, R., Riemann, R., 2009. Neurochemistry of identified motoneurons of the tensor tympani muscle in rat middle ear. Hear. Res. 248, 69–79. https://doi.org/10.1016/j.heares.2008.

Reuss, S., Siebrecht, E., Stier, U., Buchholz, H.G., Bausbacher, N., Schabbach, N., Kronfeld, A., Dieterich, M., Schreckenberger, M., 2020. Modeling vestibular compensation: neural plasticity upon thalamic lesion. Front. Neurol. 11, 441. https://doi.org/10.3389/fneur.2020.00441.

Riemann, R., Reuss, S., 1999. Nitric oxide synthase in identified olivocochlear projection neurons in rat and guinea pig. Hear. Res. 135, 181–189. https://doi.org/10.1016/s0378-5955(99)00113-6.

Ryugo, D.K., Haenggeli, C.A., Doucet, J.R., 2003. Multimodal inputs to the granule cell domain of the cochlear nucleus. Exp. Brain Res. 153, 477–485. https://doi.org/10.1007/s00221-003-1605-3.

Safieddine, S., Eybalin, M., 1992. Triple immunofluorescence evidence for the coexistence of acetylcholine, enkephalins and calcitonin gene-related peptide within efferent (olivocochlear) neurons of rats and guinea-pigs. Eur. J. Neurosci. 4, 981–992. https://doi.org/10.1111/j.1460-9568.1992.tb00124.x.

Safieddine, S., Prior, A.M., Eybalin, M., 1997. Choline acetyltransferase, glutamate decarboxylase, tyrosine hydroxylase, calcitonin gene-related peptide and opioid peptides coexist in lateral efferent neurons of rat and guinea-pig. Eur. J. Neurosci. 9, 356–367. https://doi.org/10.1111/j.1460-9568.1997.tb01405.x.

Sánchez-González, M.A., Warr, W.B., López, D.E., 2003. Anatomy of olivocochlear neurons in the hamster studied with FluoroGold. Hear. Res. 185, 65–76. https://doi.org/10.1016/s0378-5955(03)00213-2.

Schaeffer, D.F., Reuss, M.H., Riemann, R., Reuss, S., 2003. A nitrergic projection from the superior olivary complex to the inferior colliculus of the rat. Hear. Res. 183, 67–72. https://doi.org/10.1016/s0378-5955(03)00219-3.

Shen, J., Harada, N., Nakazawa, H., Yamashita, T., 2005. Involvement of the nitric oxide-cyclic GMP pathway and neuronal nitric oxide synthase in ATP-induced Ca2+ signalling in cochlear inner hair cells. Eur. J. Neurosci. 21, 2912–2922. https://doi.org/10.1111/j.1460-9568.2005.04135.x.

Singec, I., Knoth, R., Ditter, M., Hagemeyer, C.E., Rosenbrock, H., Frotscher, M., Volk, B., 2002. Synaptic vesicle protein synaptoporin is differently expressed by subpopulations of mouse hippocampal neurons. J. Comp. Neurol. 452, 139–153. https://doi.org/10.1002/cne.10371.

Steinbusch, H.W.M., 1981. Distribution of serotonin-immunoreactivity in the central nervous system of the rat - cell bodies and terminals. Neuroscience 6, 557–618. https://doi.org/10.1016/0306-4522(81)90146-9.

Sun, T., Xiao, H.S., Zhou, P.B., Lu, Y.J., Bao, L., Zhang, X., 2006. Differential expression of synaptoporin and synaptophysin in primary sensory neurons and up-regulation of synaptoporin after peripheral nerve injury. Neuroscience 141, 1233–1245. https://doi.org/10.1016/j.neuroscience.2006.05.010.

Thompson, A.M., Schofield, B.R., 2000. Afferent projections of the superior olivary complex. Microsc. Res. Tech. 51, 330–354. https://doi.org/10.1002/1097-0029(20001115)51:4<330::Aid-jemt4>3.0.Co;2-x.

Usdin, T.B., Hoare, S.R., Wang, T., Mezey, E., Kowalak, J.A., 1999. TIP39: a new neuropeptide and PTH2-receptor agonist from hypothalamus. Nat. Neurosci. 2, 941–943. https://doi.org/10.1038/14724.

Varga, T., Palkovits, M., Usdin, T.B., Dobolyi, A., 2008. The medial paralemniscal nucleus

and its afferent neuronal connections in rat. J. Comp. Neurol. 511, 221–237. https://doi.org/10.1002/cne.21829.

Wang, X., Robertson, D., 1997. Effects of bioamines and peptides on neurones in the ventral nucleus of trapezoid body and rostral periolivary regions of the rat superior olivary complex: an in vitro investigation. Hear. Res. 106, 20–28. https://doi.org/10.1016/s0378-5955(96)00211-0.

Warford, A., Akbar, H., Riberio, D., 2014. Antigen retrieval, blocking, detection and visualisation systems in immunohistochemistry: a review and practical evaluation of tyramide and rolling circle amplification systems. Methods (San. Diego, Calif.) 70, 28–33. https://doi.org/10.1016/j.ymeth.2014.03.001.

Wynne, B., Harvey, A.R., Robertson, D., Sirinathsinghji, D.J., 1995. Neurotransmitter and neuromodulator systems of the rat inferior colliculus and auditory brainstem studied by in situ hybridization. J. Chem. Neuroanat. 9, 289–300. https://doi.org/10.1016/0891-0618(95)00095-x.

Yassin, L., Radtke-Schuller, S., Asraf, H., Grothe, B., Hershfinkel, M., Forsythe, I.D., Kopp-Scheinpflug, C., 2014. Nitric oxide signaling modulates synaptic inhibition in the superior paraolivary nucleus (SPN) via cGMP-dependent suppression of KCC2. Front. Neural Circuits 8, 65. https://doi.org/10.3389/fncir.2014.00065.